Chapter 4

Hydrogen-induced Degradation

This chapter discusses several process parameters from the viewpoint of hydrogen-induced degradation. The parameters are Zr/Ti compositional ratios, $PbTiO_3$ seed layer, capacitor structures (Pt/PZT/Pt and Ir/IrO_2/PZT/Pt/IrO_2), amounts of excess Pb, and domain poling. These are very critical issues in the integration of ferroelectric capacitor modules because they are important determinants of capacitor performance. Capacitor performance can be optimized by controlling these process parameters to minimize the hydrogen-induced degradation.

§1. INTRODUCTION

One of the biggest problems that PZT ferroelectric capacitors suffer from during integration is the loss of hysteresis characteristics in an atmosphere that contains hydrogen dissociated from the precursor material, such as the passivation layer deposition and the forming gas anneal process. Such a phenomenon is referred to as hydrogen-induced degradation, hydrogen damage or hydrogen attack. There are three typical hydrogen-induced damages observed, which include the decrease of remnant polarization, increase in leakage current, and delamination of the electrodes. The ferroelectric capacitor stack should be able to withstand annealing at above 400 ^oC in hydrogen-containing ambient to realize highly reliable memory devices.

It is well known that the degradation of PZT capacitors is closely related to the electrode materials, especially top electrode [1-3]. It has been suggested that the catalytic activity of the top electrode, ability of dissociating molecular hydrogen into atomic

hydrogen, plays a critical role in the degradation of PZT capacitors. Group 10 (Ni, Pd, Pt), metals have strong catalytic activity compared to group 9 (Ir, Rh) and 11 (Ag, Au) elements. In the case of Pt, a typical electrode material for a ferroelectric capacitor, the catalytic activity is so high that hydrogen molecules would dissociate and be adsorbed chemically at low temperatures, even at 150 K, and migrate freely without an energy barrier [4,5]. Without the top electrode, a bare PZT film begins to degrade from 400 ^{o}C by the forming gas anneal. However, when the Pt top electrode is deposited, Pt/PZT/Pt capacitors begin to degrade at low temperature, even below 150 ^{o}C [6].

Miki *et al*. suggested an interfacial reduction model, which explains the degradation of electrical properties most reasonably up to the present [6]. In this model, activated hydrogen, protons or radicals, penetrate the Pt electrode into PZT, and react to reduce PZT at the Pt/PZT interface. As a result, oxygen vacancies which produce positively charged centers, could occur, thus damaging the interface. These defects pile up at the Pt/PZT interface and act as a heavily doped semi-conductive layer, resulting in a positive space charge and voltage drop. This model provides a reasonable explanation for the increase of leakage currents, and the asymmetric I-V breakdown behavior. However, there still is no model so far which can elucidate the degradation in view of the ferroelectric material itself.

The changes in PZT crystal structures caused by hydrogen-induced damage have not yet been fully elucidated. Only two papers have been published relative to this issue. Ikarashi detected phase changes near the PZT/Pt interface by TEM analysis, and concluded that the decrease in Pb composition, and distortion of Ti-O coordination were caused by forming gas anneal [7]. Aggarwal reported that hydroxyl bonds (OH^-) is formed in PZT films by the forming gas anneal, and proposed that bonded hydrogen prevents the Ti (or Zr) ion from switching [8]. Surprisingly, despite the many results on the degradation of

ferroelectric properties, PZT films still maintain their crystal structure after the forming gas anneal. On the contrary, it was reported that SBT films, rival of PZT, lost their crystal structure by the forming gas anneal [9,10].

§2. EXPERIMENTAL PROCEDURE

Two types of ferroelectric capacitor modules with the structure of Pt/PZT/Pt (100/200/270/30 nm) and Ir/IrO_2/PZT/Pt/IrO_2/TiO_2 (120/30/200/150/50/50 nm), were fabricated onto 200 nm oxidized silicon (100) substrates, with capacitor size of 100 x 100μm^2. PZT thin films, typically 200 nm in thickness, were deposited by the sol-gel technique [11]. After PZT film formation, a surface cleaning process was attempted to eliminate the possible detrimental effect of secondary phases, and to adjust the film thickness. Electrode materials (Pt, Ir, IrO_2) and adhesion layers (Ti, TiO_2) were deposited by a DC sputtering method. After the top electrode (TE) deposition, TE and PZT layers were dry etched consecutively by means of ICP (Inductively Coupled Plasma) etcher with Ar-Cl_2-C_2F_6 gas mixtures. For the study on the effect of Zr/Ti ratio in PZT films, four types of PZT precursor solutions which have constant Pb excess amount (10%) and various Zr/Ti ratios (60/40, 52/48, 40/60, 30/70) were prepared. To investigate the effect of Pb excess amount, solutions with constant Zr/Ti ratio (40/60) and various levels of excess Pb (10%, 13%, 16%, 19%) were prepared. To facilitate perovskite phase formation, the $PbTiO_3$ seed layer was employed with the thickness of about 10 nm in some case. Prior to the hydrogen anneal, a sidewall cleaning process was employed to remove the etching damaged layer formed at the side region of PZT films during the dry etching process [12]. The situation that leads to hydrogen-induced degradation during integration was reproduced by performing heat treatment in the N_2 gas ambient containing 4% H_2 (forming gas) in the temperature range 100-350 ^oC. This annealing process will be referred to as the “hydrogen anneal” in this study.

Evaluation of hysteretic properties and domain poling of PZT films were

performed using a Radiant Technologies RT66A system. The physical and chemical properties of hydrogen damaged capacitors were characterized using various analytic techniques such as secondary ion mass spectrometry (SIMS), X-ray diffraction (XRD), X-ray photoelectron spectroscopy (XPS), and scanning electron microscopy (SEM).

§3. COMPARISON OF Pt/PZT/Pt WITH $Ir/IrO_2/PZT/Pt/IrO_2$ STRUCTURES

Pt/PZT(40/60)/Pt capacitor structure (A) has been studied as a basic ferroelectric capacitor structure, because the majority of knowledge has been developed based on this structure for a last decade. This might be attributed to the ease of fabrication due to its simple structure, and the growth of high quality PZT on the Pt electrode. However, this structure has a drawback in that remnant polarization (P_r) decreases as read/write pulse cycle repeats, the so called fatigue problem. This fatigue issue can be solved easily by applying an oxide electrode. This is the main reason for why the $Ir/IrO_2/PZT/Pt/IrO_2$ capacitor structure (B) was developed. In practice, this structure has been utilized successfully for the development of 64 K FRAM and 4 M FRAM devices [13,14].

In addition to the fatigue issue, capacitor B shows a better resistance against hydrogen anneal compared with that of capacitor A as shown in figure 4-1. In capacitor A, ferroelectric switching is completely suppressed and acts as paraelectric phases when a hydrogen anneal is performed over 200 ^oC. On the other hand, capacitor B still shows switching properties even at an annealing temperature of 250 ^oC, although hysteresis loops are degraded considerably. Current characteristics of hydrogen annealed capacitors were obtained by differentiating the polarization values with respect to time (figure 4-2). In addition to the degradation of polarization, it can be observed that domain switching is delayed, or coercive voltage increases, as the temperature of hydrogen anneal increases. Capacitor A showed a constant decrease in switching current and an increase in coercive voltage. However, interestingly, capacitor B showed somewhat intricate switching behaviors, *i.e.*, an earlier domain switching of hydrogen annealed at 100 ^oC and a double switching of hydrogen annealed at 150 ^oC for periods of 5-7 *m*Sec.

The monitoring of the coercive voltage shift V_{sh} (V_c–V_{ave}), in figure 4-3, definitely indicates that the hysteresis loops shifted to the positive bias direction in the case of Pt/PZT/Pt capacitors, whereas the loops moved to the negatively bias direction in Ir/IrO_2/PZT/Pt/IrO_2. Considering the chemical reactions of the activated hydrogen and components in the ferroelectric capacitor module, thermodynamic data indicates that IrO_2 has the highest standard reduction potential with PbO being next as shown in table 4-1. From the SIMS depth profile of hydrogen atoms in both capacitors (figure 4-4), we can predict what types of chemical reactions occurred and where the reactions took place during the hydrogen anneal. In the case of Pt/PZT/Pt capacitors PbO has the highest reduction potential, this implies that both sides of the PZT interfaces is the tentative location of a reduction reaction. However as shown in figure 4-4, hydrogen atoms were mainly piled up at the top Pt/PZT interface, although a small hump can be seen at the PZT/bottom Pt interface. It is thought that the difference in the hydrogen amount at both interfaces developed a built-in potential, thus causing the shifts of hysteresis loops in the positive bias direction. The asymmetric piling of hydrogen atoms could be attributed to interface strength, since PZT film growth follows a heterogeneous mechanism in sol-gel deposition, therefore the PZT/bottom Pt interface should be stronger than the top Pt/PZT interface. The bottom Pt/PZT interface undergoes the same thermal budget of high temperature annealing, but the top Pt is deposited on a PZT film surface at low temperature. Moreover excess PbO which is added to facilitate perovskite formation, gathers in the top surface of PZT films, thus enhancing the reaction with hydrogen at the top Pt/PZT interface.

On the contrary, similar amounts of hydrogen were observed at both sides of the PZT interfaces in the case of Ir/IrO_2/PZT/Pt/IrO_2 capacitors, and hysteresis loops shifted to the negative bias direction (figure 4-3 and 4-4). IrO_2 has the highest reduction potential in this capacitor module, and therefore, the major fraction of hydrogen piled up in IrO_2/PZT interface as a result of preferential reaction with IrO_2, thereby allowing the shift to negative direction. The major cause of the coercive voltage shift lies in the reduction of PbO which exists at the PZT/bottom Pt interface in this structure. In practice, the reduction of IrO_2 is so serious that delamination occurs at the Pt/IrO_2 interface even hydrogen anneal

temperature of 100 ^{o}C and blister formation is observed at the Ir/IrO_2 interface for cases of hydrogen anneals above 250 ^{o}C (Figure 4-5). On the other hand, in the case of the Pt/PZT/Pt capacitor, the top Pt/PZT interface is always delaminated. The mechanism of Pt/PZT interface delamination is discussed in chapter 6.

Table 4-1. Standard Reduction Potential $E^{Ø}$ (V) (298K, 1 atm) [15,16]

Material	Chemical Reaction	Standard Potential (V)
TiO_2	$TiO_2 + 4H \rightarrow Ti + 2H_2O$	$E^{Ø} = -2.132$
ZrO_2	$ZrO_2 + 4H \rightarrow Zr + 2H_2O$	$E^{Ø} = -1.456$
PbO	$PbO + 2H \rightarrow Pb + H_2O$	$E^{Ø} = 0.248$
IrO_2	$IrO_2 + 4H \rightarrow Ir + 2H_2O$	$E^{Ø} = 0.926$

Assuming that the space charge distribution, incorporated hydrogen, represents the major cause of coercive voltage shift, the built-in potential is maximum 0.7 V. The trapped charge density can be estimated by

$$Q = CV_{in} = \varepsilon_0 \varepsilon E_{in}$$

Where C is capacitance, ε_0 is the permittivity of vacuum, and ε is the dielectric constant of the PZT(40/60) film. For the Pt/PZT(40/60)/PZT capacitors the dielectric constant ε= 670, the trapped charge density becomes 2.1$\mu C/cm^2$, which is about 4.2% of $2P_r$ value. This value corresponds to about 1.3 x 10^{13} electron/cm^2 accumulated at the interface.

§4. DEPENDENCE OF PZT FILM COMPOSITION

The components in PZT films such as Zr/Ti ratio, $PbTiO_3$ seed layer, and excess

amount of PbO are critical parameters which play a role in the performance of PZT capacitors. The Zr/Ti ratio is most critical factor because it is directly related to hysteretic properties such as coercive voltage and polarization values. As the Ti component increases, the squareness in hysteresis loop is enhanced which is a positive factor, but it also has a drawback in that the coercive voltage increases. The degradation trends of remnant polarization indicate that the hydrogen-induced degradation is intensified in Ti-rich PZT capacitors as shown in figure 4-6. The SIMS depth profile, figure 4-7, clearly shows that the amount of hydrogen accumulated at the interface is increased as the Ti portion increases in PZT films. Another example also supports this trend, when the $PbTiO_3$ seed layer is used in PZT film growth. Usually the introduction of the a $PbTiO_3$ seed layer lowers the crystallization temperature and facilitates the formation of films which are free of secondary phases [17]. The seed layer could be placed either upside or downside of the PZT film. When these films were exposed to hydrogen anneal, as shown in figure 4-8, the most rapid degradation was observed when the $PbTiO_3$ seed layer was employed at the top Pt/PZT interface. Based on above results, it is likely that PZT films easily lose their polarization properties as a result of the hydrogen anneal, since the Ti portion increase in PZT films. There is no clear explanation for this finding, but it is assumed that Ti participate in the reduction reaction indirectly, since the standard reduction potential of TiO_2 is the highest among the components in a ferroelectric capacitor module.

The PbO content of the PZT films has been widely recognized as affecting not only the phase assembly and microstructure but also the dielectric and ferroelectric properties. Excess PbO has been usually incorporated in PZT films to optimize the film properties by compensating for PbO loss either through volatilization or diffusion into the substrate [18]. Sol-gel derived PZT(40/60) films with various excess Pb contents (10%, 13%, 16%, 19%) were prepared and utilized to fabricate $Ir/IrO_2/PZT/Pt/IrO_2$ capacitors. After the hydrogen anneal at 300 ^oC for 5 min, the degree of the hydrogen incorporation was analyzed by the SIMS technique. As shown in figure 4-9, more hydrogen was detected when PZT contains a higher excess PbO content.

Although PZT capacitors completely lost their ferroelectric switching properties

and behaved like a paraelectric material after a hydrogen anneal above 300 ^{o}C, XRD patterns indicated that the perovskite structure was still maintained as shown in figure 4-10. In addition, we were not able to detect any changes in chemical states in hydrogen annealed PZT films by XPS analysis. In figure 4-11, the dielectric constants exhibit gradual degradation as the hydrogen anneal temperature goes up, reaching saturated values about 50-60% of initial values. Electrical measurements of capacitors which have been hydrogen annealed at temperatures over 350 ^{o}C was impossible because the electrodes were so seriously delaminated. Therefore it is thought that activated hydrogen reacts with PbO, and form hydroxyl groups (OH), thereby decreasing dielectric constants and switching polarization values. The existence of hydroxyl groups in perovskite film has already been conclusively demonstrated [8,19]. Of course, if the hydrogen anneal is performed at a very high temperature, the PZT film would be reduced to pure metals. However it seems that only a partial reduction can occur in the temperature range of the standard silicon processes which utilize hydrogen-containing precursors.

§5. DEPENDENCE OF THE POLING STATE

Prior to the hydrogen anneal, Pt/PZT/Pt capacitors were electrically poled by applying +5V and –5V separately. This experiment was originally intended to investigate the nature of the activated hydrogen, neutral radicals, positive charged protons, or negative charged hydride ions. Considering the electronegativitiy of the electrode materials (Pt: 2.28, Ir: 2.20) and hydrogen (H: 2.20), the activated hydrogen would not exist as a proton or a hydride. According to an early study, it appears that the Pt dissolves hydrogen molecules without hydride formation [20]. If protons are the origin of the hydrogen-induced degradation, the +5V poling should speed up the degradation, because the negative dipole developed at top Pt/PZT interface would be expected to enhance the approach of the protons. As shown in figure 4-12 and 4-13, however, the degradation was retarded by the +5V application. Therefore it is assumed that the activated hydrogen take the character of neutral radicals.

As discussed in an earlier section, a negative charge should be developed at the top Pt/PZT interface as the activated hydrogen appears, because hysteresis loops are moved to the positive bias direction. If negative dipole was developed at the interface by applying +5V, the hydrogen-induced degradation (or reduction reaction) could be suppressed because the negative dipole served to prevent the negative charge buildup. Further study will be required to understand clearly why negatively (-5V) poled capacitors show slower P_r degradation trends compared to unpoled capacitors. The experimental results can be applied to FRAM production in order to reduce hydrogen-induced degradation. By applying positive voltage (write '0') prior to plastic packaging, one of the major processes producing the hydrogen-induced degradation as a final step of device production, we can expect minimal degradation in the hysteretic properties.

§6. SUMMARY AND MODEL SUGGESTION

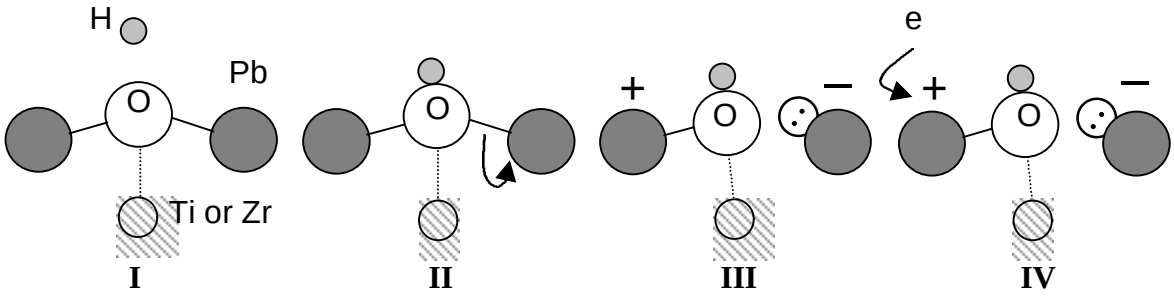

We have investigated several process parameters in terms of hydrogen-induced degradation. The parameters are very critical in determining the performance of ferroelectric capacitors, such as Zr/Ti compositional ratios, electrode structures (Pt/PZT/Pt and $Ir/IrO_2/PZT/Pt/IrO_2$), excess amounts of Pb, and the domain poling state. It was found that the hydrogen-induced degradation is enhanced when PZT films have high Ti and Pb compositions, and can be suppressed by domain poling prior to the hydrogen anneal. From a SIMS analysis and hysteresis loop shifts, it can be concluded that the hydrogen damage occurs mainly at the PZT/electrode interface and results in the development of negative

charge buildup.

Based on above results, hydrogen-induced degradation can occur as a result of hydroxyl formation. After the dissociation of hydrogen molecules, activated hydrogen, probably neutral radicals, diffuse into the electrode/PZT interface (**I**), and react with PbO, since it has the highest standard reduction potential (**II**). Due to the new bond formation between oxygen and hydrogen atoms, the Pb-O bond breaks (**III**). Both negative and positive charges might be developed in Pb atoms separately. Positively charged Pb is very unstable because the orbital has an unpaired electron, thus easily attracting electrons from the electrode, but negative charged Pb is relatively stable because its orbital is occupied by paired electrons (**IV**). The chemical reaction between hydrogen and PbO makes the negative charge development in Pb atoms and degrades the hysteresis characteristics.

§7. REFERENCES

[1] Jin-Ping Han, T. P. Ma, *Appl. Phys. Lett*. **71** (9), 1267 (1997)

[2] Y. Shimamoto, K. Kushida-Abdelghafar, J. Miki, and Y. Fujisaki, *Appl. Phys. Lett*. **70** (23), 3096 (1997)

[3] Yoshihisa Fujisaki, Keito Kushida-Abdelghafar, Yasuhiro Shimamoto, and Hiroshi Miki, *J. Appl. Phys*. **82** (1), 341 (1997)

[4] K. Christman, G. Ertl, and T. Pignet, *Surface Science* **54**, 365 (1976)

[5] H. Nakatsuji, Y. Matsuzaki, and T. Yonezawa, *J. Chem. Phys*. **88** (9), 5759 (1988)

[6] Hiroshi Miki, Keito Kushida-Abdelghafar, Kazuyoshi Torii, and Yoshihisa Fujisaki, Jpn. *J. Appl. Phys*. **36** (3A), 1132 (1997)

[7] Nobuyuki Ikarashi, *Appl. Phys. Lett*. **73** (14), 1955 (1998)

[8] S. Aggarwal, S. R. Perusse, C. W. Tipton, R. Ramesh, H. D. Drew, T. Venkatesan, D. B. Romero, V. B. Podobedov, and A. Weber, *Appl. Phys. Lett*. **73** (14), 1973 (1998)

[9] Sufi Zafar, Vidya Kaushik, Paul Laberge, Peir Chu, Robert E. Jones, Robert L. Hance,

Peter Zurcher, Bruce E. White, Deborah Taylor, Bradly Melnick, and Sherry Gillespie, *J. Appl. Phys*. **82** (9), 4469 (1997)

[10] Takashi Hase, Takehiro Noguchi, and Yoichi Miyasaka, *Integrated Ferroelectrics* **16**, 29 (1997)

[11] Wan In Lee, June Key Lee, Jong Sik Lee and In Kyeong Yoo, *Integrated Ferroelectrics* **10**, 145 (1995)

[12] June Key Lee, Tae-Young Kim, Ilsub Chung and Seshu. B. Desu, *Appl. Phys. Lett*. **75** (3), 334 (1999)

[13] D. J. Jung, S. Y. Lee, B. J. Koo, Y. S. Hwang, D. W. Shin, J. W. Lee, Y. S. Chun, S. H. Shin, M. H. Lee, H. B. Park, K. Kim and J. G. Lee, *VLSI Tech. Symp*., 122 (1998)

[14] S. Y. Lee, D. J. Jung, Y. S. Song, B. J. Koo, S. O. Park, H. J. Cho, S. J. Oh, D. S. Hwang, J. K. Lee, Y. S. Park, I. S. Chung, K. Kim, *VLSI Tech. Symp*., 141 (1999)

[15] David R. Lide, *CRC Handbook of Chemistry and Physics*, 71th Ed. 1990-1991

[16] Marcel Poarbaix, *Atlas of Electrochemical Equilibria in Aquous Solution*, 2nd Ed. National Association of Corrosion Engineers, 1974

[17] Kenji Ishikawa, Kazunari Sakura, Desheng Fu, Shiro Yamada, Hisao Suzuki, and Takashi Hayashi, *Jpn. J. Appl. Phys*. **37** (9B), 5128 (1998)

[18] G. Teowee, J. M. Boulton, K. McCarthy, E. K. Franke, T. P. Alexander, T. J. Bukowski and D. R. Uhlmann, *Integrated Ferroelectrics* **14**, 265 (1997)

[19] Gyu-Chul Yi, and Bruce W. Wessels, *Appl. Phys. Lett*. **71** (3), 327 (1997)

[20] M.W. Roberts, and C. S. Mckee, *Chemistry of the metal-gas interface*, Clarenson, Oxford, 383 (1978)

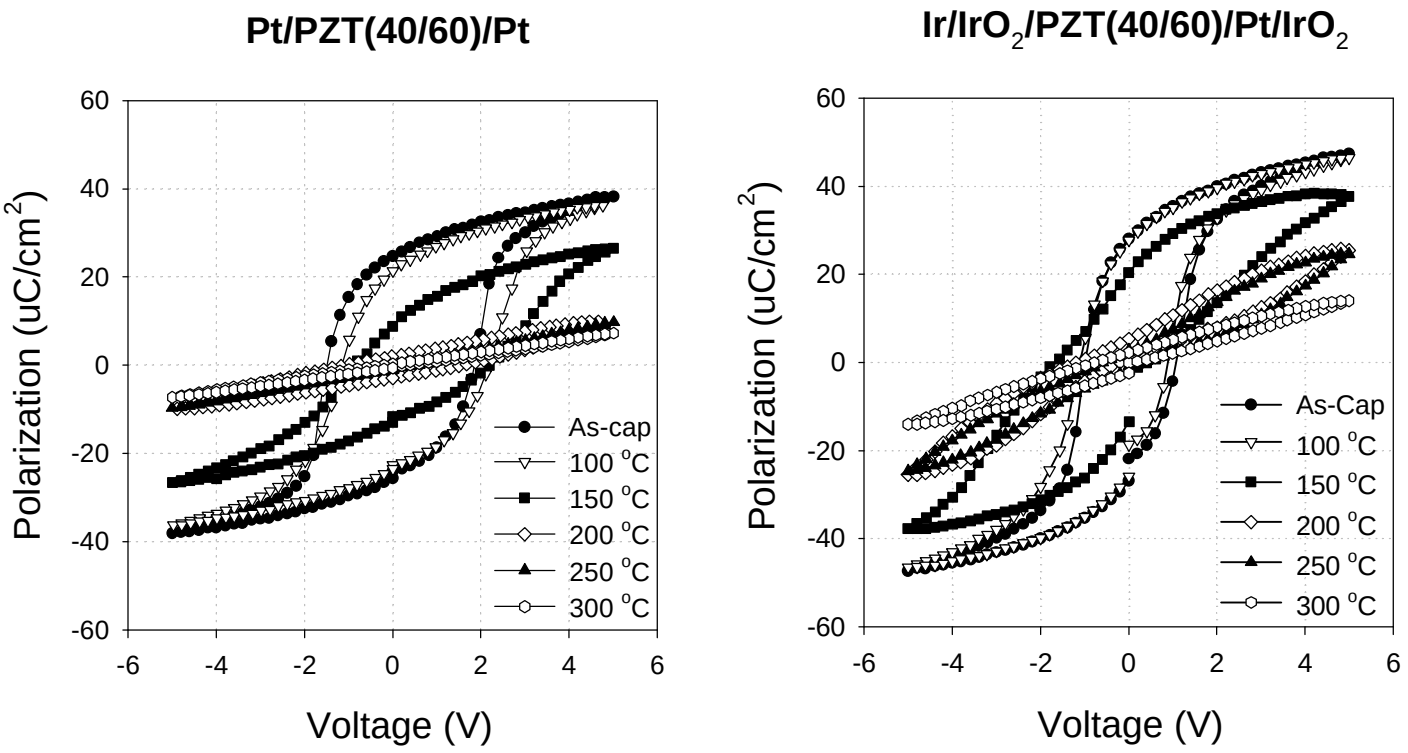

Figure 4-1. Hysteresis loops of Pt/PZT/Pt and Ir/IrO_2/PZT/Pt/IrO_2. Both capacitors were exposed to a hydrogen anneal for 5 min in the temperature range 100-300 ^{o}C.

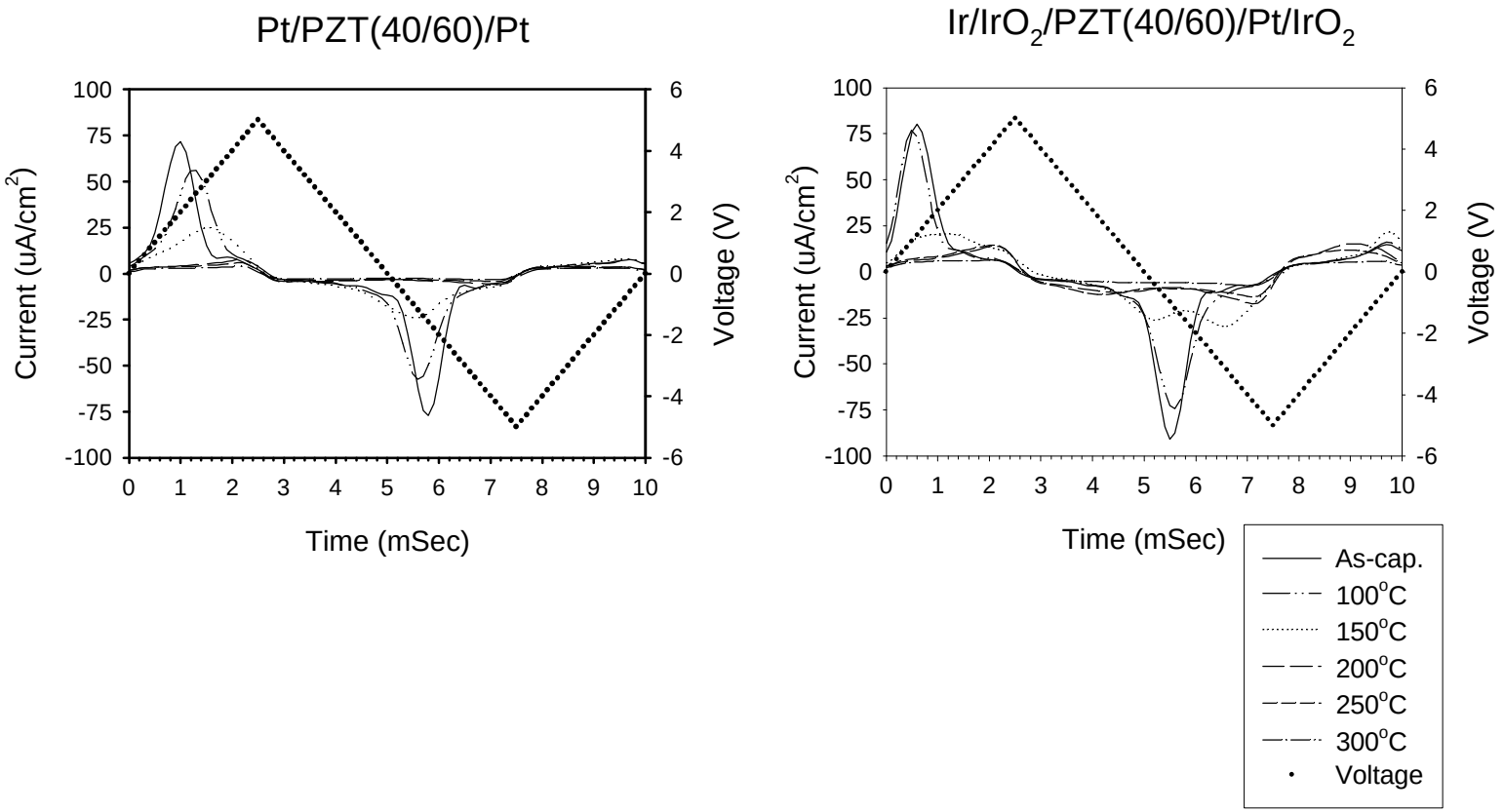

Figure 4-2. Currents from domain switching in hydrogen damaged Pt/PZT/Pt and Ir/IrO_2/PZT/Pt/IrO_2 capacitors.

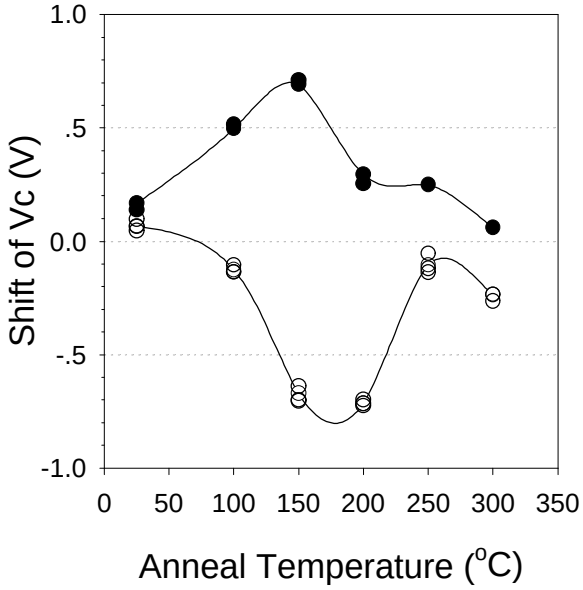

Figure 4-3. Shifts of coercive voltage in hydrogen damaged capacitors. Pt/PZT(40/60)/Pt (●), Ir/IrO_2/PZT(40/60)/Pt/IrO_2 (○)

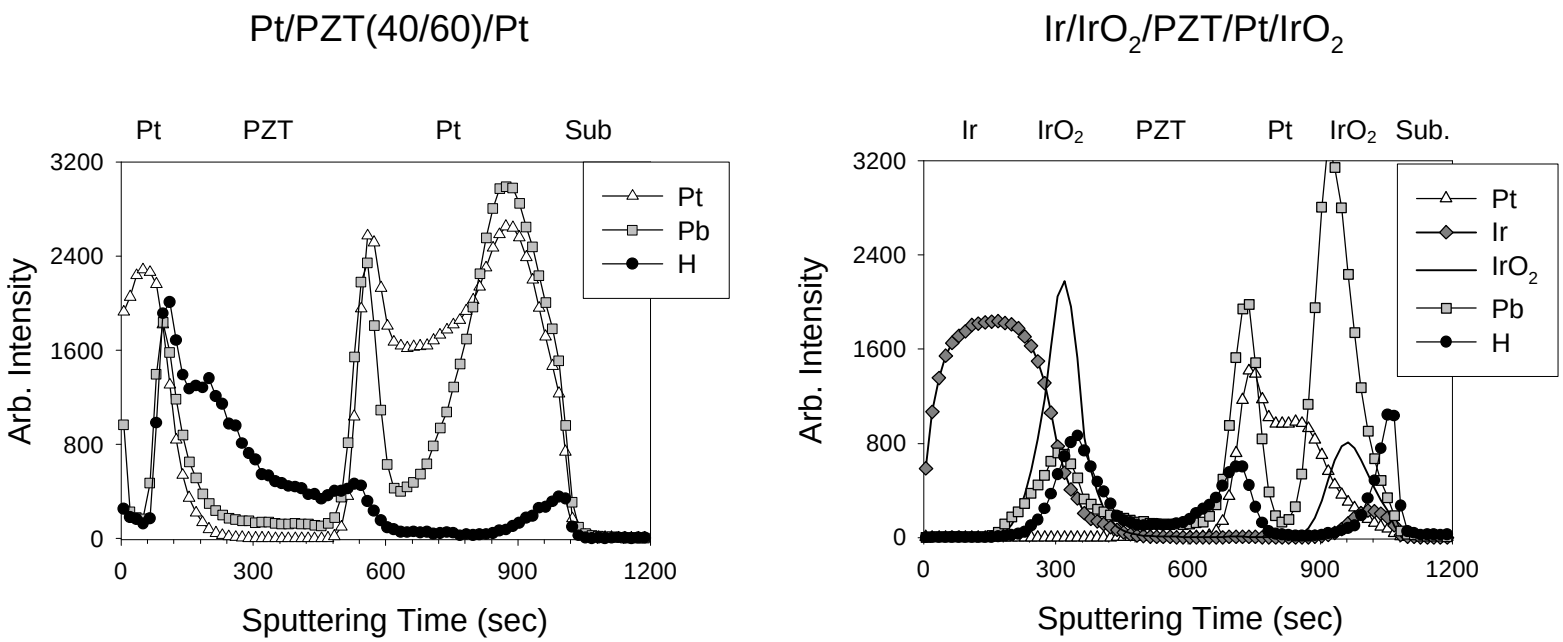

Figure 4-4. SIMS depth profiles of hydrogen damaged Pt/PZT/Pt and Ir/IrO_2/PZT(40/60)/Pt/IrO_2 capacitors

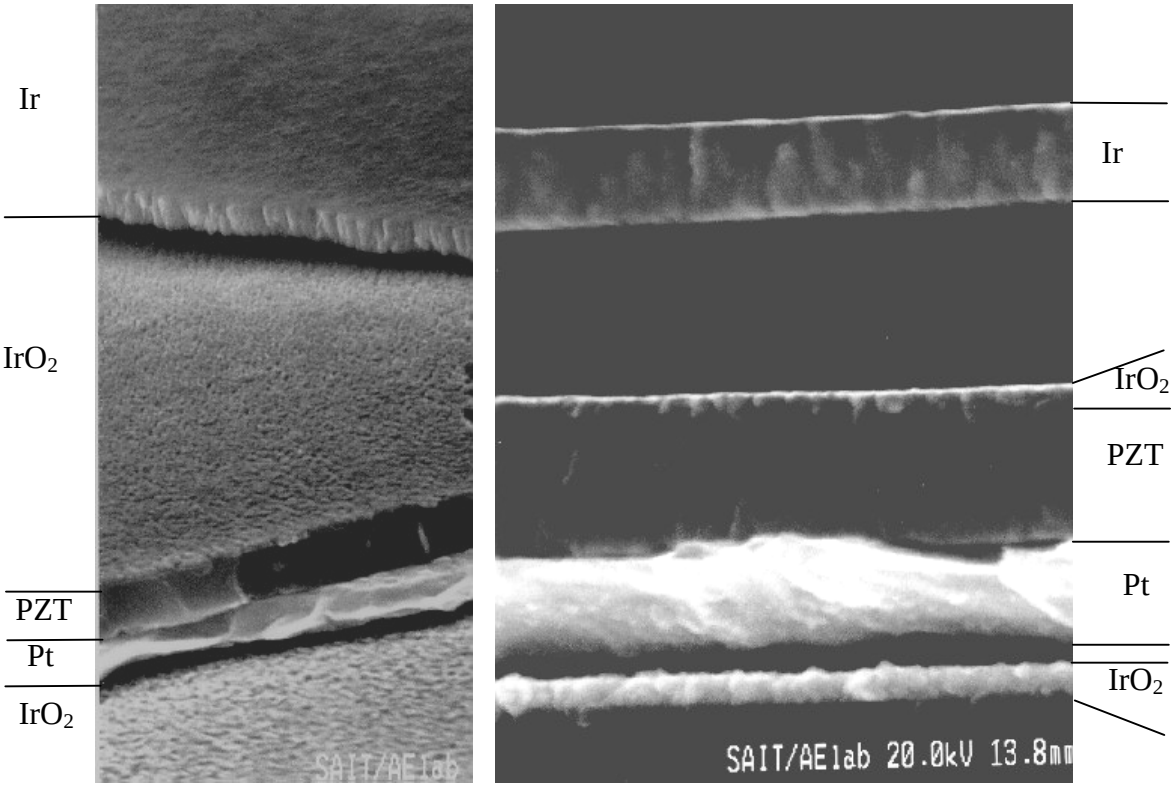

Figure 4-5. SEM photograhps of hydrogen annealed Ir/IrO_2/PZT(40/60)/Pt/IrO_2. Delamination has clearly occurred at the interfaces between Ir/IrO_2 and Pt/IrO_2.

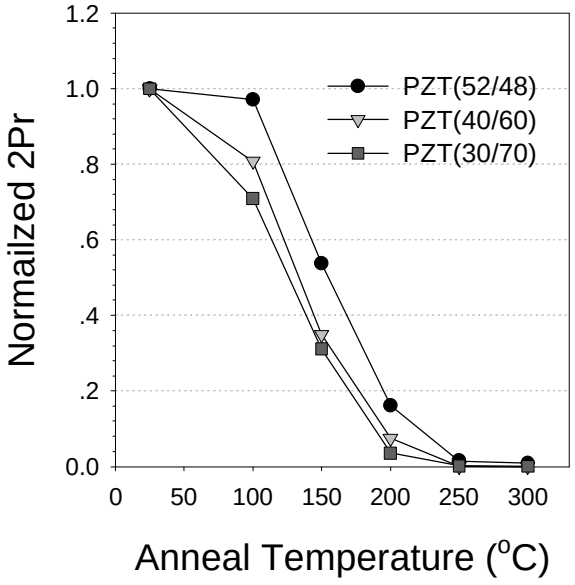

Figure 4-6. Degradation of remnant polarization by hydrogen annealing with variation in Zr/Ti composition.

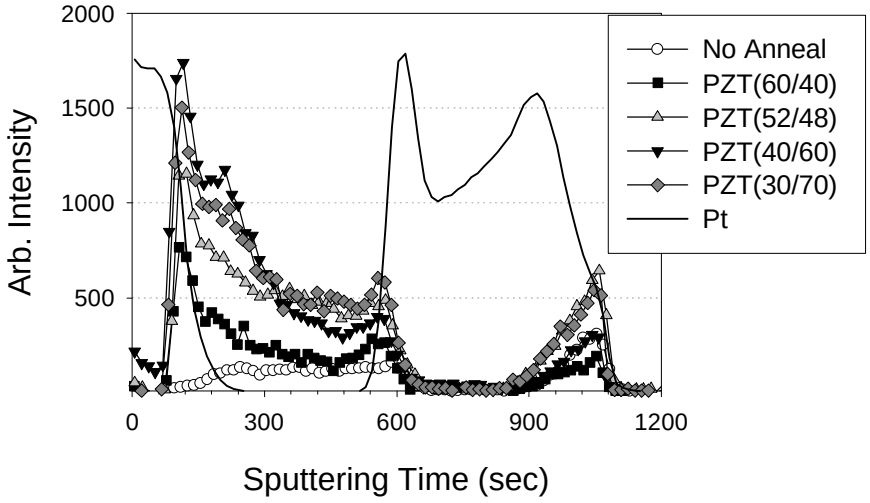

Figure 4-7. SIMS depth profile of hydrogen atom in Pt/PZT/Pt capacitors which have various Zr/Ti composition (60/40, 52/48, 40/60, 30/70). Hydrogen anneal was performed at 150^{o}C for 5 min.

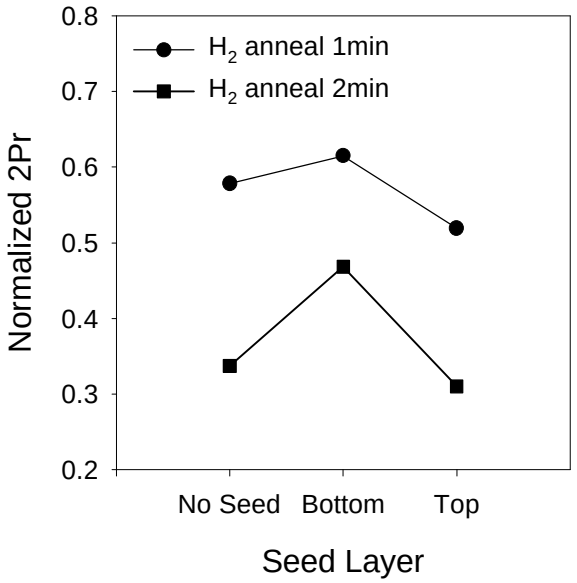

Figure 4-8. Degradation of remnant polarization for the $PbTiO_3$ seed layer (thickness ~100Å) is applied to enhance a crystallinity. Hydrogen anneal was performed at 200 ^oC. The structure of capacitors was PT/PZT(52/48)/Pt.

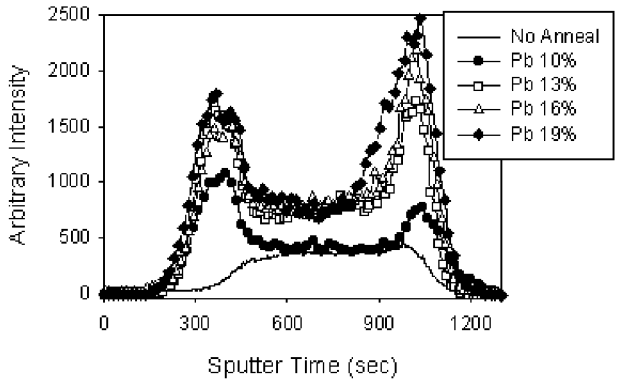

Figure 4-9. SIMS depth profile of hydrogen atom in $Ir/IrO_2/PZT(40/60)/Pt/IrO_2$ capacitors which contain different levels of excess Pb. Hydrogen anneal was performed at 300 ^oC for 5 min.

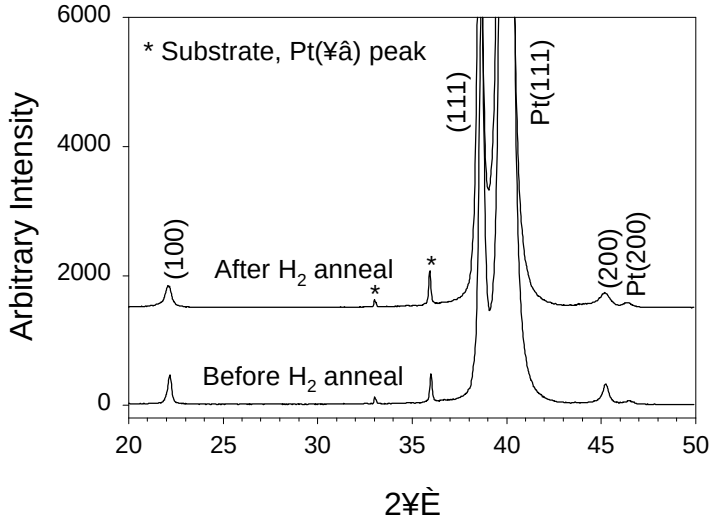

Figure 4-10. XRD diffraction pattern of Pt/PZT(40/60)/Pt before and after hydrogen anneal. Hydrogen anneal was performed at 300 ^{o}C for 5 min.

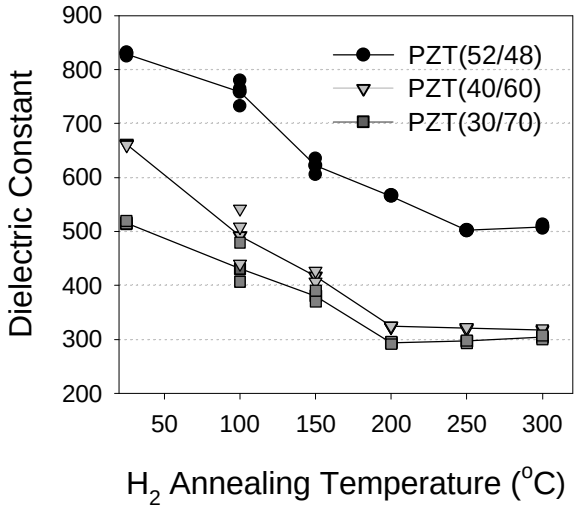

Figure 4-11. Degradation of dielectric constant of PZT films by hydrogen anneal.

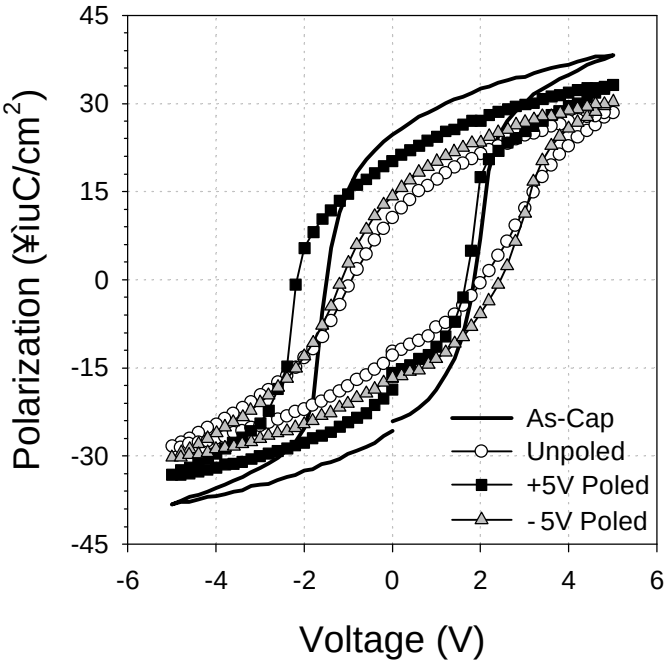

Figure 4-12. Hysteresis loops of Pt/PZT(40/60)/Pt capacitors, which were hydrogen annealed at 100 ^{o}C for 125 min. Prior to the hydrogen anneal, capacitors were poled by ±5V triangular pulse.

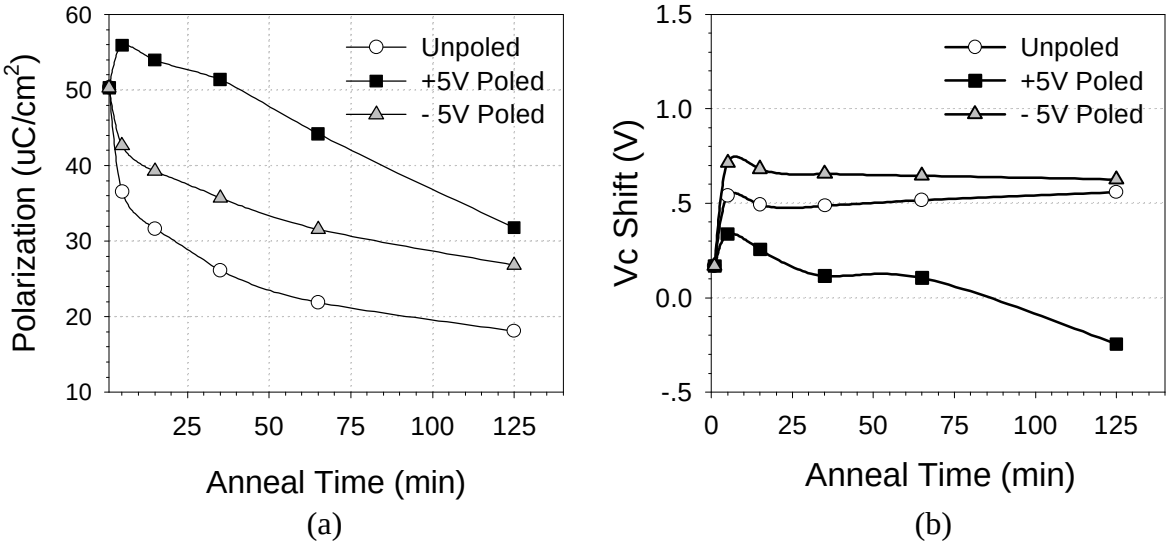

Figure 4-13. Variation in hysteretic properties in hydrogen annealed Pt/PZT(40/60)/Pt capacitors. (a) Remnant polarization ($2P_r$) and coercive voltage (V_c). The hydrogen anneal was performed at 100 ^{o}C.